0026-895X/08/7303-960–967$20.00
MOLECULAR PHARMACOLOGY
Copyright © 2008 The American Society for Pharmacology and Experimental Therapeutics
Mol Pharmacol 73:960–967, 2008

Vol. 73, No. 3
42481/3309508
Printed in U.S.A.

Atomic Force Microscopy Reveals the Stoichiometry and Subunit Arrangement of the $\alpha_4\beta_3\delta$ $GABA_A$ Receptor

Nelson P. Barrera, Jill Betts, Haitao You, Robert M. Henderson, Ian L. Martin, Susan M. J. Dunn, and J. Michael Edwardson

Department of Pharmacology, University of Cambridge, Cambridge, United Kingdom (N.P.B., J.B., R.M.H., J.M.E.); Department of Pharmacology, and Centre for Neuroscience, University of Alberta, Edmonton, Canada (H.Y., S.M.J.D.); and School of Life and Health Sciences, Aston University, Birmingham, United Kingdom (I.L.M.)

Received October 4, 2007; accepted December 12, 2007

ABSTRACT

The $GABA_A$ receptor is a chloride-selective ligand-gated ion channel of the Cys-loop superfamily. The receptor consists of five subunits arranged pseudosymmetrically around a central pore. The predominant form of the receptor in the brain contains α_1-, β_2-, and γ_2-subunits in the arrangement $\alpha\beta\alpha\gamma\beta$, counter-clockwise around the pore. $GABA_A$ receptors containing δ- instead of γ-subunits, although a minor component of the total receptor population, have interesting properties, such as an extrasynaptic location, high sensitivity to GABA, and potential association with conditions such as epilepsy. They are therefore attractive targets for drug development. Here we addressed the subunit arrangement within the $\alpha_4\beta_3\delta$ form of the receptor. Different epitope tags were engineered onto the three subunits, and complexes between receptors and anti-epitope antibodies were imaged by atomic force microscopy. Determination of the numbers of receptors doubly decorated by each of the three antibodies revealed a subunit stoichiometry of 2α:2β:1δ. The distributions of angles between pairs of antibodies against the α- and β-subunits both had peaks at around 144°, indicating that these pairs of subunits were nonadjacent. Decoration of the receptor with ligands that bind to the extracellular domain (i.e., the lectin concanavalin A and an antibody that recognizes the β-subunit N-terminal sequence) showed that the receptor preferentially binds to the mica extracellular face down. Given this orientation, the geometry of complexes of receptors with both an antibody against the δ-subunit and Fab fragments against the α-subunits indicates a predominant subunit arrangement of $\alpha\beta\alpha\delta\beta$, counter-clockwise around the pore when viewed from the extracellular space.

The $GABA_A$ receptor, responsible for fast inhibitory transmission in the central nervous system, is a member of the Cys-loop ligand-gated ion channel superfamily, together with the nicotinic acetylcholine receptor, the $5\text{-}HT_3$ receptor, and the glycine receptor (Karlin, 2002; Lester et al., 2004). The receptor exists as a heteromeric complex of five subunits, arranged pseudo-symmetrically around a central Cl^- ion channel (Sieghart, 1995). Electron microscopy of samples of purified $GABA_A$ receptor reveals a cylinder of external diameter 7 nm with a central pore of diameter 2 to 3 nm (Nayeem et al., 1994). Nineteen $GABA_A$ receptor subunit isoforms have so far been identified (Barnard et al., 1998). The predominant form of the receptor in the brain contains α_1-, β_2-, and γ_2-subunits in the stoichiometry 2α:2β:1γ (Farrar et al., 1999). Previous work, in which various combinations of concatenated subunits were expressed in *Xenopus laevis* oocytes, indicated a subunit arrangement of $\alpha\beta\alpha\gamma\beta$, reading counter-clockwise around the pore when viewed from the extracellular face of the membrane (Baumann et al., 2002; Baur et al., 2006).

It is now clear that $GABA_A$ receptors are found not only at the synapse but also extrasynaptically, where they act as sensors for extracellular GABA, mediating tonic inhibition (Brickley et al., 2001; Nusser and Mody, 2002; Stell et al., 2003). A significant population of extrasynaptic receptors seems to contain at least one δ-subunit, in combination with α_4- or α_6- and β_1- or β_3-subunits (Nusser et al., 1998; Brickley et al., 2001; Nusser and Mody, 2002; Stell et al., 2003). The δ-containing receptors are particularly sensitive to the natural agonist GABA, the response to which shows no evidence of the positive cooperativity that is displayed by the most ubiquitous member of the family comprising α_1-, β_2- and γ_2-subunits; the δ-containing receptors also desensitize significantly more slowly (Brown et al., 2002). Viewed from a pharmacological perspective, the δ-containing receptors lack sensitivity to the classic benzodiazepines, and THIP is a more

This work was supported by grants from the Biotechnology and Biological Sciences Research Council (B19797) (to J.M.E. and R.M.H.) and from the Canadian Institute of Health Research (to S.M.J.D. and I.L.M.).
Article, publication date, and citation information can be found at http://molpharm.aspetjournals.org.
doi:10.1124/mol.107.042481.

ABBREVIATIONS: AFM, atomic force microscopy; HA, hemagglutinin; CHAPS, 3-[(3-cholamidopropyl)dimethylammonio]-1-propanesulfonate

efficacious agonist than GABA (Adkins et al., 2001; Brown et al., 2002; Chandra et al., 2006; Stórustovu and Ebert, 2006). Although the expression of the δ-subunit is restricted in both density and distribution, there is evidence that both exogenous and endogenous stimuli result in significant plastic changes in its expression. Decreases in the level of expression of δ-containing receptors have been found in various animal models of epilepsy (Schwarzer et al., 1997; Zhang et al., 2007), and increases have been observed in mice during adolescence (Shen et al., 2007) and in rats during late diestrus (Lovick et al., 2005), suggesting potential roles for these receptors in epilepsy, emotional stress in teenagers, and premenstrual psychological disturbances in women. Thus, although the δ-containing receptors represent only a minor component of the total $GABA_A$ receptor population, their atypical properties render them attractive novel targets for drug development. Exploration of receptor attributes at the molecular level has been facilitated by the construction of homology models of the $\alpha_1\beta_2\gamma_2$ receptor, using the nicotinic acetylcholine receptor as the structural template (Ernst et al., 2005; Mokrab et al., 2007). However, because recognition sites for agonists, antagonists, and allosteric agents are found at subunit interfaces within this family, it is important to determine not only the stoichiometry but also the architecture of the subunits within the pentamer if useful homology models are to be constructed for other receptor subtypes. We have developed a method, based on atomic force microscopy (AFM) imaging, for directly determining the arrangement of subunits within multimeric proteins. So far, we have applied this method to the architecture of the $\alpha_1\beta_2\gamma_2$ $GABA_A$ receptor (Neish et al., 2003), the 5-HT_3 receptor (Barrera et al., 2005a), and the P2X receptor (Barrera et al., 2005b, 2007). The method involves engineering epitope tags onto the receptor subunits and expressing the receptors exogenously in a suitable cell line (tsA 201). Receptors isolated from the transfected cells are then incubated with antibodies to the tags, and the resulting receptor-antibody complexes are imaged by AFM. The geometry of the complexes reveals the receptor architecture. We have used this method to determine the subunit arrangement within the $\alpha_4\beta_3\delta$ $GABA_A$ receptor.

Materials and Methods

$GABA_A$ Receptor Subunit Constructs. The rat cDNA sequences used in these studies were those reported in the NCBI database: α_4, NM_080587; β_3, NM_017065.1; and δ, NM_017289. cDNA encoding the $GABA_A$ receptor α_4-subunit, with a C-terminal FLAG epitope tag, was subcloned into the vector pcDNA3.1/V5-His A using HindIII and AgeI, so as to delete the V5 epitope tag. cDNA encoding the β_3-subunit, was subcloned into the same vector using KpnI and XbaI. cDNA encoding the $GABA_A$ receptor δ-subunit with a C-terminal HA epitope tag was subcloned intothe same vector using KpnI and AgeI, so as to delete the V5 epitope tag.

Transient Transfection of tsA 201 Cells. Transfections of tsA 201 cells (a subclone of human embryonic kidney 293 cells stably expressing the simian virus 40 large T-antigen) were carried out using the CalPhos mammalian transfection kit (Clontech, Mountain View, CA). After transfection, cells were incubated for 24 to 48 h at 37°C, to allow expression of the receptors.

Solubilization and Purification of His_6-Tagged Receptors. The solubilization/purification procedure was as described previously for P2X receptors (Barrera et al., 2005b). In brief, a crude membrane fraction prepared from transfected tsA 201 cells was solubilized in 1% (w/v) 3-[(3-cholamidopropyl)dimethylammonio]-1-propanesulfonate, and the solubilized material was incubated with Ni^{2+}-agarose beads (Probond; Invitrogen, Carlsbad, CA). The beads were washed extensively, and bound protein was eluted with increasing concentrations of imidazole. Samples were analyzed by SDS-polyacrylamide gel electrophoresis, and protein was detected by immunoblotting, using mouse monoclonal antibodies against the His_6 tag, present on all subunits (Research Diagnostics Inc., Flanders, NJ), the FLAG tag on the α_4-subunit (Sigma, St. Louis, MO), the V5 tag on the β_3-subunit (Invitrogen), or the HA tag on the δ-subunit (Covance Research Products, Princeton, NJ), as appropriate. An anti-Myc antibody (Roche Applied Science, Indianapolis, IN) was used as a negative control.

AFM Imaging of Receptors and Receptor-Antibody Complexes. $GABA_A$ receptors were imaged either alone or after incubation for 14 h at 4°C with a 1:2 molar ratio (approximately 0.2 nM receptor concentration) of either anti-FLAG, anti-V5, anti-HA, or anti-His_6 monoclonal antibodies. An anti-Myc antibody (Roche Applied Science) was used as a negative control. Receptors were also incubated with Fab fragments of the anti-FLAG antibody, generated by papain digestion (ImmunoPure Kit; Pierce, Rockford, IL). Proteins were diluted to a final concentration of 0.04 nM, and 45 μl of the sample was allowed to adsorb to freshly cleaved, poly-L-lysine-coated mica coverslips (Sigma). After a 10-min incubation, the sample was washed with MilliQ-water and dried under nitrogen. Imaging was performed with a Multimode atomic force microscope (Digital Instruments, Santa Barbara, CA). Samples were imaged in air, using tapping mode. The silicon cantilevers used (MikroMasch, Madrid, Spain) had a drive frequency of ~300 kHz and a specified spring constant of 40 N/m. The applied imaging force was kept as low as possible (target amplitude of ~1.6–1.8 V and amplitude setpoint of ~1.3–1.5 V).

The molecular volumes of the protein particles were determined from particle dimensions based on AFM images. After adsorption of the receptors onto the mica support, the particles adopted the shape of a spherical cap. The heights and half-height radii were measured, and the molecular volume was calculated using the following equation: $V_m = (\pi h/6)(3r^2 + h^2)$, where h is the particle height and r is the radius (Schneider et al., 1998).

Molecular volume based on molecular mass was calculated using the equation $V_c = (M_0/N_0)(V_1 + dV_2)$, where M_0 is the molecular mass, N_0 is Avogadro's number, V_1 and V_2 are the partial specific volumes of particle and water, respectively, and d is the extent of protein hydration (Schneider et al., 1998).

Results

Exogenous Expression of $\alpha_4\beta_3\delta$ $GABA_A$ Receptors. Rat $\alpha_4\beta_3\delta$ $GABA_A$ receptors were expressed in tsA 201 cells by transfection with the appropriate cDNAs. The α_4-subunit bore a FLAG-His_6 tag; the β_3-subunit bore a V5-His_6 tag, and the δ-subunit bore a hemagglutinin- (HA-)His_6 tag. All tags were at the C-termini of the subunits. In cells transfected with cDNAs for all three subunits (at a 1:1:1 ratio by weight), anti-His_6, anti-FLAG, anti-V5, and anti-HA antibodies all gave positive immunofluorescence signals, but an anti-Myc antibody was negative (Fig. 1A). In cells transfected with cDNA for the β_3- and δ-subunits, the anti-FLAG antibody antibody gave no signal, as expected. Likewise, the anti-V5 antibody gave no signal in cells transfected with the α_4- and δ-subunits, and the anti-HA antibody gave no signal in cells transfected with the α_4- and β_3-subunits. These results indicate that all three subunits are expressed in the tsA 201 cells and are detected specifically by the appropriate anti-epitope antibodies. The receptors were located both at the plasma membrane and in internal membranes.

Receptor Isolation. Crude membrane fractions of the transfected cells were solubilized in the detergent CHAPS (1%), and the receptors were isolated through their binding to Ni^{2+}-agarose columns via their His_6 tags. As shown in Fig. 1B, the isolated $GABA_A$ receptor gave positive signals on immunoblots with anti-FLAG, anti-V5, and anti-HA antibodies. The major bands in all three lanes ran at 50 to 60 kDa in size order $\alpha_4 > \beta_3 > \delta$, consistent with the expected sizes of the three subunits and their previously reported mobilities on gels (Bencsits et al., 1999). An anti-Myc antibody gave no signal with the isolated receptor; furthermore, none of the antibodies gave a signal with fractions isolated from mock-transfected cells. These results show that the isolation procedure used results in the production of receptors containing all three subunits. The double bands seen in the lanes showing the α_4-, β_3-, and δ-subunits probably represent different glycosylation states. It has been shown that inhibition of *N*-linked glycosylation by tunicamycin does not affect receptor assembly (Connolly et al., 1996). Hence, the presence of subunits at various stages of glycosylation is unlikely to influence the results of our experiments.

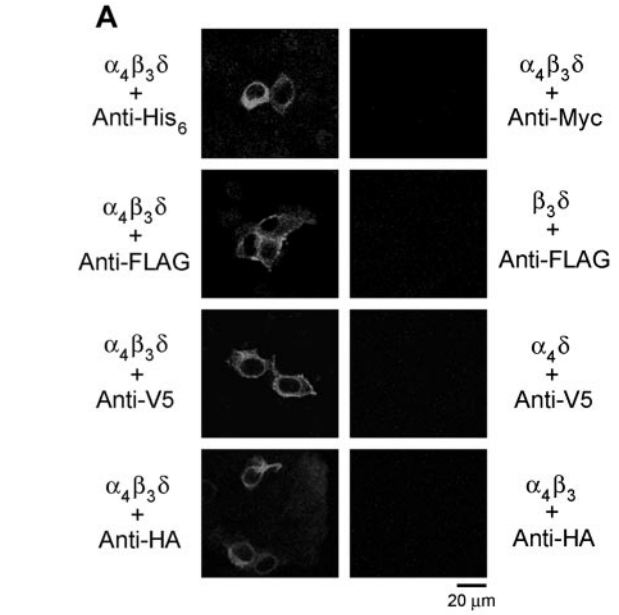

Fig. 1. Immunofluorescence and immunoblot analysis of $GABA_A$ receptors. A, immunofluorescence detection of $GABA_A$ receptors in transfected tsA 201 cells. Cells were transfected with the cDNA for various combinations of subunits. They were then fixed, permeabilized, and incubated with monoclonal primary antibodies, followed by a Cy3-conjugated goat anti-mouse secondary antibody. Cells were imaged by confocal laser scanning microscopy. B, detection of $GABA_A$ receptors in eluates from Ni^{2+}-agarose columns. Samples from either transfected or mock-transfected cells were analyzed by SDS-polyacrylamide gel electrophoresis and immunoblotting, using monoclonal anti-FLAG, anti-V5, anti-HA, and anti-Myc primary antibodies followed by a horseradish peroxidase-conjugated goat anti-mouse secondary antibody. Immunoreactive bands were visualized using enhanced chemiluminescence. Arrows indicate receptor subunits, and arrowheads indicate molecular mass markers (kilodaltons).

AFM Imaging of Receptors. The $GABA_A$ receptor preparation was adsorbed to a mica support, dried, and subjected to AFM imaging in air. In a control experiment, a sample from mock-transfected cells was imaged. As shown in Fig. 2A, this sample was almost featureless. In contrast, the $GABA_A$ receptor population appeared as a spread of particles (Fig. 2B). The difference in the appearances of the samples from mock-transfected and transfected cells indicates that the vast majority of the imaged particles represent isolated receptors or receptor subunits. The heights and radii of a large number of receptor particles from each sample were determined, as described previously (Neish et al., 2003; Barrera et al., 2005a,b, 2007). Particle radii were measured at half the maximal height to compensate for the tendency of AFM to overestimate this parameter when the radii of both particle and scanning tip are similar (i.e., in the nanometer range; Schneider et al., 1998). The dimensions were used to calculate molecular volumes using the equation $V_m = (\pi h/6)(3r^2 + h^2)$. The frequency distribution of the calculated molecular volumes (Fig. 2C) had two clear peaks, at 120 ± 4 nm^3 (mean ± S.E.M.; $n = 431$) and 593 ± 31 nm^3 ($n = 110$). Each particle in Fig. 2B can be assigned based on its size to one of the two peaks, an arbitrary division being

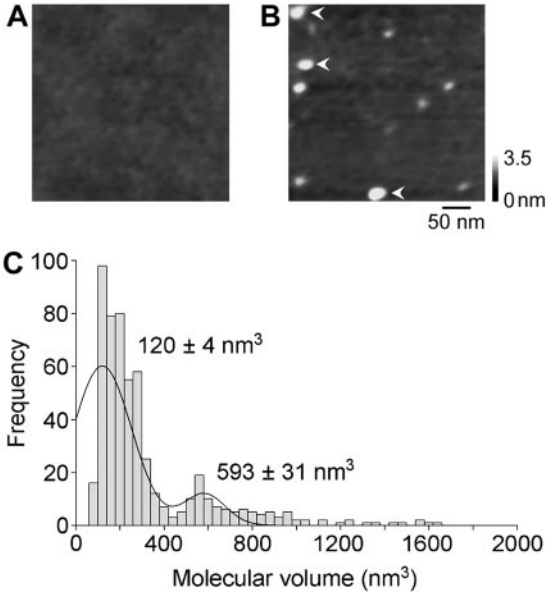

Fig. 2. AFM imaging of $GABA_A$ receptors. A, image of a sample prepared from mock-transfected cells. B, image of a sample from cells transfected with the cDNA for all three $GABA_A$ receptor subunits. Arrowheads indicate particles with a molecular volume >420 nm^3; the remaining particles (unmarked) are <420 nm^3. A shade-height scale is shown at the right. C, frequency distribution of molecular volumes of $GABA_A$ receptors. The curve indicates the fitted double-Gaussian function. The distribution was arbitrarily divided at a molecular volume of 420 nm^3, to calculate the errors on the means.

made at 420 nm^3. Arrowheads indicate particles with a molecular volume >420 nm^3; the remaining particles (unmarked) are <420 nm^3. Clearly, the larger molecular volume (593 nm^3) is approximately five times the smaller molecular volume (120 nm^3), suggesting that the two peaks correspond to monomers and pentamers. The predicted molecular volume of a $GABA_A$ receptor subunit [according to the equation $V_c = (M_0/N_0)(V_1 + dV_2)$], based on a molecular mass of 55 kDa, is 105 nm^3, close to the measured volume of 120 nm^3. This close correspondence suggests that the particles imaged are indeed $GABA_A$ receptor subunits and pentameric receptors. The small discrepancy between the predicted and the measured volumes is probably accounted for by the presence of some detergent bound to the isolated proteins, as has been observed for other ionotropic receptors (Neish et al., 2003; Barrera et al., 2005a,b, 2007).

Determination of the Subunit Stoichiometry by AFM Imaging of Receptor-Antibody Complexes. The $GABA_A$ receptor was next imaged after incubation with mouse monoclonal antibodies against its epitope tags—FLAG on the α_4-subunit, V5 on the β_3-subunit, HA on the δ-subunit, and His_6 on all three subunits. As shown in Fig. 3A, the receptor alone appeared as a heterogeneous spread of

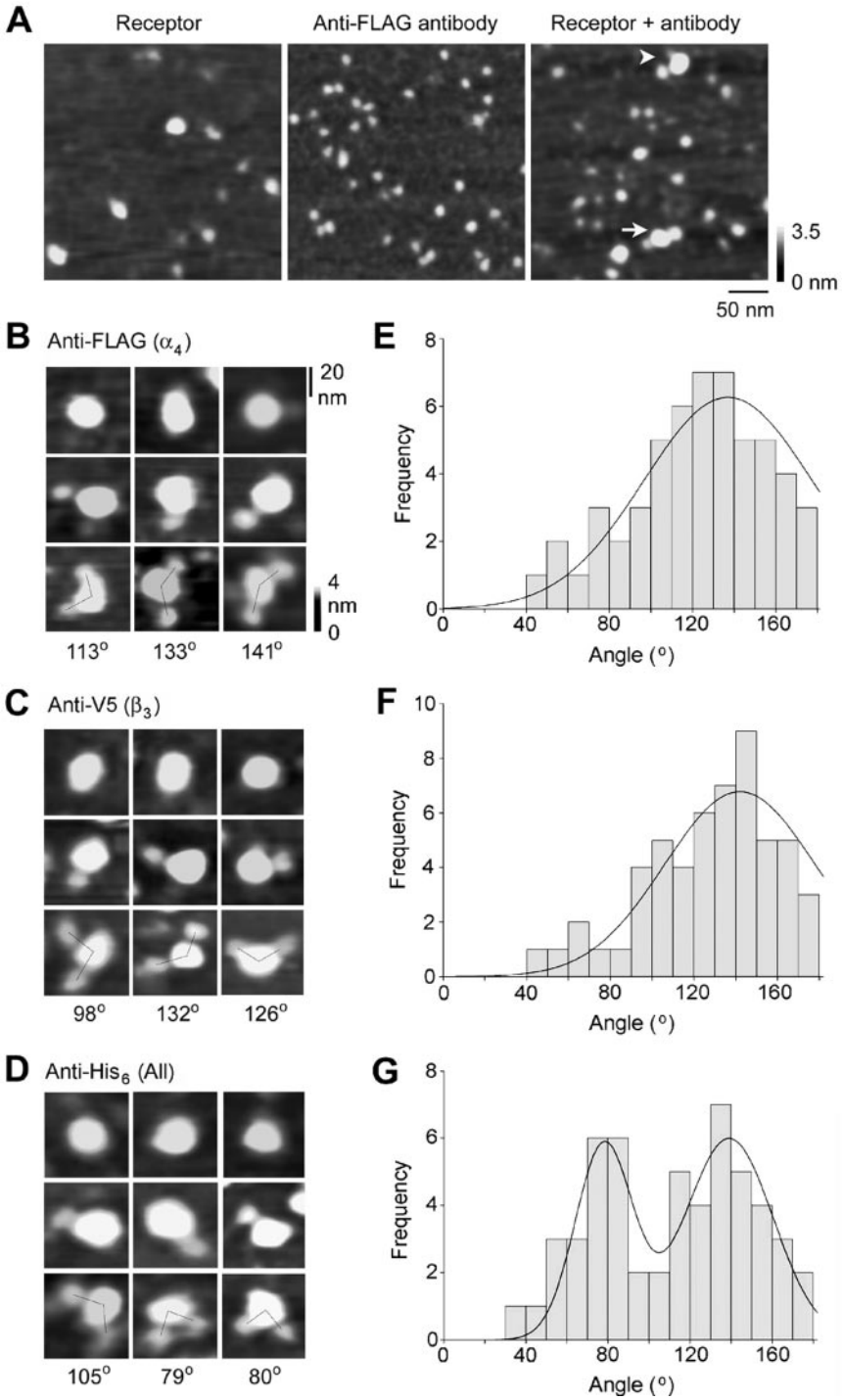

Fig. 3. AFM imaging of complexes between $GABA_A$ receptors and anti-subunit antibodies. A, images of receptors (left), anti-FLAG antibodies (middle), and receptor-antibody complexes (right). B–D, zoomed images of receptors that are uncomplexed (top), or bound by one (middle) or two (bottom) anti-FLAG (B), anti-V5 (C), or anti-His_6 (D) antibodies. A shade-height scale is shown at the right. E–G, frequency distributions of angles between anti-FLAG (E), anti-V5 (F) or anti-His_6 (G) antibodies. The curve indicates the fitted single (E and F) or double (G) Gaussian functions. In G, the distribution was arbitrarily divided at an angle of 105° to calculate the errors on the means.

particles. Anti-FLAG antibody samples showed a more homogenous population of particles, as expected. Samples resulting from coincubations of receptors and anti-FLAG antibodies appeared very heterogeneous. Nevertheless, there were examples of large particles (molecular volume >420 nm^3) that were decorated by one (arrowhead) or two (arrows) smaller particles (presumably antibodies). Figure 3, B–D, shows galleries of images of individual receptors, either undecorated or decorated with one or two anti-FLAG (Fig. 3B), anti-V5 (Fig. 3C), and anti-His_6 (Fig. 3D) antibodies. For each anti-epitope antibody, many datasets were analyzed and the status (i.e., undecorated, singly decorated, or double-decorated) of the larger (>420 nm^3) particles was assessed (Table 1). To ensure that the apparent receptor-antibody complexes were genuine and not simply a consequence of large and small particles settling close together on the mica surface, a control experiment was carried out in which the receptor was incubated with an anti-Myc antibody. In this case, 2.0% of 248 large particles appeared to have one small particle attached, and only one large particle appeared to be doubly decorated by small particles. In contrast, when the receptors were incubated with anti-FLAG, anti-V5, anti-HA, or anti-His_6 antibodies, a substantial proportion (25.7–32.8%) of the large particles were decorated by single antibodies. It is noteworthy that the proportion of the large particles that were doubly decorated by antibodies was in the range 7.1 to 7.8% for the anti-FLAG, anti-V5, and anti-His_6 antibodies but was much smaller (0.7%) for the anti-HA antibody. These results indicate that the subunit stoichiometry of the receptor is 2α:2β:1δ.

Given a 2α:2β:1δ stoichiometry, there are six possible arrangements of subunits, reading counter-clockwise around the receptor rosette: $\alpha\beta\alpha\delta\beta$, $\alpha\beta\alpha\beta\delta$, $\alpha\alpha\beta\beta\delta$, $\alpha\alpha\delta\beta\beta$, $\alpha\delta\alpha\beta\beta$, and $\alpha\alpha\beta\delta\beta$. Note that the first two of these arrangements are mirror images of each other, and that the last four have either the two α-subunits or the two β-subunits (or both) adjacent. To narrow down the possible arrangements, receptors decorated with two anti-FLAG, anti-V5, or anti-His_6 antibodies were identified, and the angles between the pairs of bound antibodies were calculated by joining the height peaks of the particles. The angles were used to construct the frequency distributions shown in Fig. 3, E–G. For both anti-FLAG and anti-V5 antibodies, the distributions had single peaks, at 137 ± 4° (mean ± S.E.M.; $n = 54$) and 142 ± 4° ($n = 54$), respectively, indicating that both the α- and the β-subunits were separated by another subunit (expected angle 144°). In contrast, the angle distribution for the anti-His_6 antibody, which should bind to all three types of subunit, had two peaks, at 78 ± 4° ($n = 23$) and 139 ± 3° ($n = 31$), indicating that it was binding to either adjacent or nonadjacent subunits. Based on these results, the last four subunit arrangements (above) can be ruled out, leaving two remaining possibilities: $\alpha\beta\alpha\delta\beta$ and $\alpha\beta\alpha\beta\delta$.

Determination of the Subunit Arrangement. To determine the absolute subunit arrangement, we used two different approaches in tandem: 1) decoration of the receptor simultaneously with recognizably different ligands for either α- and δ- or β- and δ-subunits, and 2) determination of the orientation of the receptor on the mica substrate. As a first step, we produced Fab fragments of the anti-FLAG antibody, using papain digestion. When receptors were incubated with these Fab fragments, receptor-Fab complexes were produced. A frequency distribution for angles between pairs of bound Fabs is shown in Fig. 4A. The distribution has a single peak, at 135 ± 5° ($n = 41$), again indicating that the α-subunits are nonadjacent. We then incubated the receptors with both anti-FLAG Fabs and anti-HA antibodies, to decorate both α- and δ-subunits. We identified 14 receptors that had clearly been decorated with two Fabs and one antibody. Representative images are shown in Fig. 4B along with the subunit arrangements indicated by the patterns of decoration. Note that the Fabs are smaller than the antibodies, as expected. For each of the 14 complexes, we determined the progression of angles between bound ligands, beginning with the whole antibody (bound to the δ-subunit) and reading counter-clockwise around the receptor. The angles from whole antibody to Fab, and from Fab to Fab, for individual decorated receptors are shown in Fig. 4C. The mean angles are 83° for antibody-Fab and 122° for Fab-Fab; furthermore, the Fab-Fab angles are larger than the antibody-Fab angles for 11 of the 14 pairs. A nonparametric Mann-Whitney test revealed that the Fab-Fab angle is significantly larger than the antibody-Fab angle ($P < 0.05$). These results indicate that the receptors had a preferred orientation on the mica and that the predominant subunit arrangement was $\alpha\beta\alpha\beta\delta$, counter-clockwise.

To determine the orientation of the receptors, we coated the mica with either poly-L-lysine (as usual) or poly-L-glutamate, to give either a positively or a negatively charged surface. We then bound receptors to the two surfaces and incubated them with either concanavalin A, which should bind to the oligosaccharides on the extracellular face of the receptor (Im et al., 1989), or monoclonal antibody bd17, which recognizes an epitope at the N terminus of the β-subunit (Richards et al., 1987). We reasoned that changing the charge of the mica surface would change the predominant orientation of the receptors, depending on the charge distribution over the receptor surface. According to the sequence database, the α_4-subunit has three consensus glycosylation sites. Mapping the sequence of the α_4-subunit onto a model of the structure of the $\alpha_1\beta_2\gamma_2$ form of receptor (Mokrab et al., 2007) indicates that these sites are 0.7, 2.6, and 4.7 nm from the most extracellular part of the protein. The β_3-subunit also has three consensus glycosylation sites, which are 1.4, 1.6, and 7.0 nm from the most extracellular part of the receptor. Finally,

TABLE 1
Antibody tagging profile of the $GABA_A$ receptor

Number of Particles Bound to Receptor	Anti-FLAG	%	Anti-V5	%	Anti-HA	%	Anti-His_6	%	Anti-myc	%
0	511	67.1	461	64.9	488	69.2	394	56.9	242	97.6
1	196	25.7	194	27.3	211	29.9	227	32.8	5	2.0
2	54	7.1	54	7.6	5	0.7	54	7.8	1	0.4
3	1	0.1	1	0.1	1	0.1	12	1.7	0	0.0
4	0	0.0	0	0.0	0	0.0	5	0.7	0	0.0
5	0	0.0	0	0.0	0	0.0	1	0.1	0	0.0

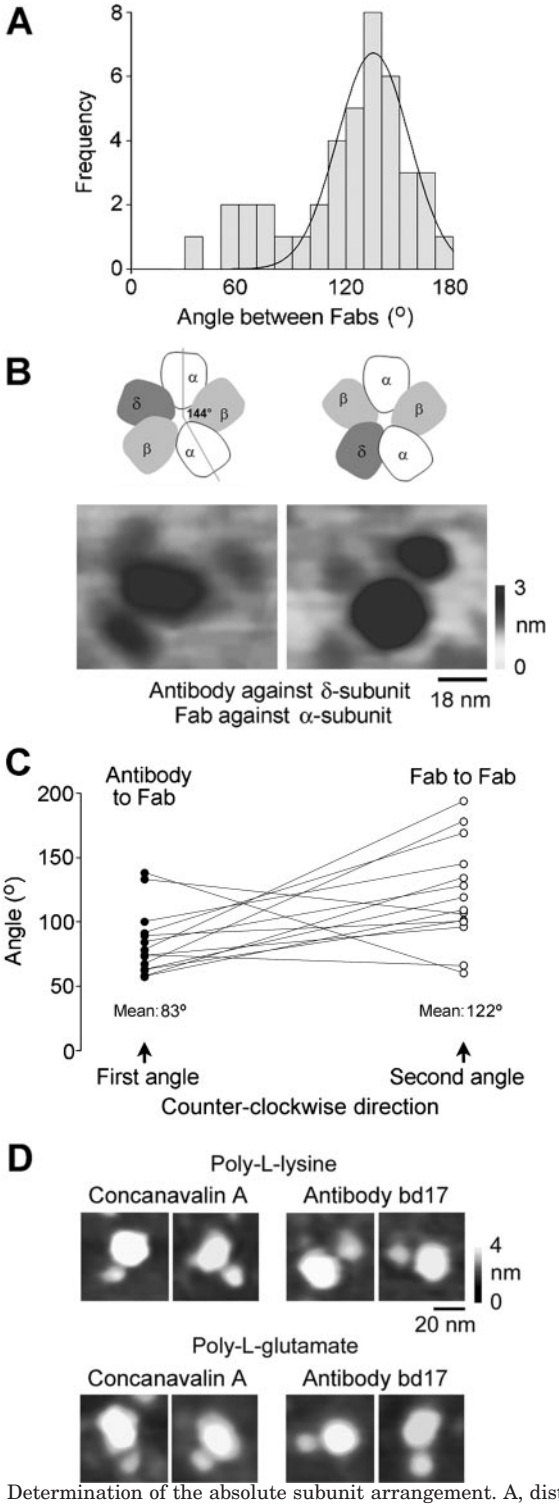

Fig. 4. Determination of the absolute subunit arrangement. A, distribution of angles between pairs of anti-FLAG Fab fragments, bound to the α-subunits. B, representative images of receptors decorated with two anti-FLAG Fab fragments and one anti-HA antibody. The left image indicates a subunit arrangement of $\alpha\beta\alpha\delta\beta$, counter-clockwise, and the right image indicates an arrangement of $\alpha\beta\alpha\beta\delta$, counter-clockwise. The two subunit arrangements are illustrated above the corresponding AFM images. C, progression of angles around the receptor for 14 receptors decorated with two Fabs and one antibody. The angles are read counter-clockwise around the receptor, beginning at the δ-subunit, which is decorated by the anti-HA antibody. Lines connect pairs of angles for individual decorated receptors. The mean angles, 83° from antibody-Fab and 122° from Fab-Fab, indicate a predominant subunit arrangement of $\alpha\beta\alpha\beta\delta$, counter-clockwise. D, representative images of receptors that had been bound to mica coated with either poly-L-lysine (top) or poly-L-glutamate (bottom) and then decorated with either concanavalin A (left) or antibody bd17 (right).

the δ-subunit has two consensus glycosylation sites, which are 1.2 and 1.5 nm from the most extracellular part of the receptor. Assuming a subunit stoichiometry of $2\alpha:2\beta:1\delta$, therefore, there are 14 potential glycosylation sites, 10 of which are within 2.6 nm of the most extracellular part of the receptor. Concanavalin A, a tetramer of molecular mass 102 kDa, has a molecular diameter of approximately 8 nm ($2 \times 0.483 \times$ (molecular mass)$^{0.386}$ (Venturoli and Rippe, 2005). Hence, we would assume that only the four sites that are either 4.7 or 7.0 nm from the most extracellular part of the receptor could possibly become tagged if the receptor were bound extracellular face down. Hence, receptors bound in this orientation would have the majority of their binding sites for concanavalin A occluded, reducing the probability of receptor decoration by the lectin. Their binding sites for antibody bd17 would also be occluded. Receptors decorated with smaller particles were observed after incubation with either concanavalin A or antibody bd17, irrespective of the mica coating. The decorated receptors shown in Fig. 4D are presumably resting on their sides, allowing the ligand to attach to the extracellular face. As shown in Table 2, for concanavalin A, 18 of 154 receptors were tagged at least once when bound to poly-L-lysine, compared with 37 of 180 when bound to poly-L-glutamate. According to the χ^2 test, the proportion of receptors tagged by concanavalin A was significantly larger for poly-L-glutamate-coated mica than for poly-L-lysine-coated mica ($P < 0.05$). Likewise, for antibody bd17, 14 of 161 receptors were tagged when bound to poly-L-lysine, compared with 37 of 217 when bound to poly-L-glutamate. Once again, the χ^2 test indicates that the proportion of receptors tagged by antibody bd17 was significantly larger for poly-L-glutamate-coated mica than for poly-L-lysine-coated mica. Hence, more extracellular faces were occluded when the mica was coated with poly-L-lysine. We conclude that the receptor normally binds predominantly extracellular face down to poly-L-lysine-coated mica, probably because the negatively charged oligosaccharides bind to the positively charged surface. In contrast, when the surface is coated with poly-L-glutamate, the receptor binds preferentially intracellular face-down, probably because the intracellular domain of this receptor carries a net positive charge (+54 for the stoichiometry described above; the charge totals are α4: 2 Asp, 8 Glu, 10 Arg, 13 Lys; β3: 10 Asp, 5 Glu, 12 Arg, 12 Lys; δ: 5 Asp, 5 Glu, 11 Arg, 9 Lys). With a receptor bound mainly extracellular face-down, the tagging pattern seen with the anti-α-subunit Fabs and the anti-δ-subunit antibody (above) indicates a predominant subunit arrangement of $\alpha\beta\alpha\delta\beta$, counter-clockwise, when viewed from the extracellular space, with some 21% (i.e., 3 of 14) of the population exhibiting a distinct subunit arrangement.

Discussion

The $\alpha_4\beta_3\delta$ $GABA_A$ receptor appears in our samples as a mixed population of assembled receptors and single subunits. The distribution of imaged particles between the two molecular volume peaks indicates that 20% of the particles are assembled receptors; put another way, 56% of the total subunits are present in assembled receptors. Whether the unassembled subunits are isolated in this state from the

transfected cells, or whether receptors undergo partial disassembly during isolation, is unclear. It has been shown previously that exogenous expression of α_1-subunits results in the production of monomers that remain in the ER and are quickly degraded (Connolly et al., 1996). In contrast, coexpression of both α_1- and β_2-subunits allowed the production of assembled receptors that accessed the cell surface. Assembly of other Cys-loop receptors, such as the nicotinic receptor (Green and Claudio, 1993), also occurs in the endoplasmic reticulum soon after polypeptide synthesis. If the $\alpha_4\beta_3\delta$ receptor behaves similarly, it is likely that, even though we are using a crude membrane fraction as our starting material and are therefore isolating receptors from intracellular membranes as well as the plasma membrane, we will be isolating a mixture of correctly assembled receptors and unassembled subunits; however, we have no information about the relative extents of these two populations. It should be noted that the unassembled subunits seen here were not seen in our previous AFM imaging studies on the $\alpha_1\beta_2\gamma_2$ $GABA_A$ receptor (Neish et al., 2003) and the 5-HT_3 receptor (Barrera et al., 2005a). This might suggest that the $\alpha_4\beta_3\delta$ receptor is particularly unstable and partially disassembles during isolation. Alternatively, one of the three subunits might be produced in excess, despite the use of equal amounts of the three cDNAs for the transfections, leading to the generation of a pool of subunits that cannot be incorporated into assembled receptors. Recent studies have suggested that the surface expression of α_1- and β_2-subunit oligomers in HEK293T cells is reduced nearly 10-fold by coexpression of the δ-subunit; maximal expression of the δ-subunits occurred at α_1:β_2:δ cDNA ratios of 1:1:0.1 (Botzolakis et al., 2007), suggesting that the appearance of single subunits in our study may indeed be associated with inefficient receptor assembly caused by the presence of the δ-subunit.

The stoichiometry of the $\alpha_4\beta_3\delta$ receptor subtype is 2:2:1, and the α- and β-subunits are nonadjacent. Simultaneous decoration of receptors with anti-α-subunit Fab fragments and an anti-δ-subunit whole antibody revealed that the receptor has a predominant subunit arrangement of $\alpha\beta\alpha\delta\beta$, in a counter-clockwise direction when viewed from the extracellular space. This arrangement is the same as that of the abundant $\alpha_1\beta_2\gamma_2$ receptor, except for the γ-δ subunit substitution. Because agonist activation sites are predicted to lie at the β-α interfaces, both receptors would have two such sites. It should be noted, however, that of the 14 receptor-antibody complexes analyzed here (Fig. 4C), three (21%) have a Fab-Fab angle smaller than the antibody-Fab angle, suggesting that a minority of the receptors might have the alternative counter-clockwise arrangement $\alpha\beta\alpha\beta\delta$ when viewed from the extracellular space, which would yield only a single agonist recognition site.

Hill slopes for GABA activation of the $\alpha_4\beta_3\delta$ receptor show no evidence of positive cooperativity, in contrast to those for the most ubiquitous $\alpha_1\beta_2\gamma_2$ receptor (Stórustovu and Ebert, 2006; Derry et al., 2007; You and Dunn, 2007). It was, therefore, an attractive possibility that differences in Hill slopes might be explained by alternative subunit arrangements of the $\alpha_4\beta_3\delta$ and $\alpha_1\beta_2\gamma_2$ receptors and hence differences in the number of agonist binding sites. However, because the predominant forms of the two receptor subtypes have the same subunit stoichiometry and arrangement, it must be their unique subunit compositions that underlie their distinct GABA activation properties.

Understanding of the molecular determinants of the recognition and functional characteristics of the "classic" $GABA_A$ receptor, $\alpha_1\beta_2\gamma_2$, has benefited significantly from the development of comparative homology models (Ernst et al., 2005; Mokrab et al., 2007). The elucidation of the subunit arrangement in the $\alpha_4\beta_3\delta$ subtype provides an opportunity to develop similar models for this receptor subtype, the importance of which in the control of neuronal excitability is becoming increasingly recognized (Farrant and Nusser, 2005). As for the $\alpha_1\beta_2\gamma_2$ $GABA_A$ receptor (Baumann et al., 2002; Baur et al., 2006), the *Torpedo californica* nicotinic receptor (Karlin et al., 1983) and the 5-HT_3 receptor (Barrera et al., 2005a), the subunits of the $\alpha_4\beta_3\delta$ receptor are apparently arranged in a preferred order to produce an assembled receptor. In contrast, it is possible to change the subunit stoichiometry of the $\alpha_4\beta_2$ nicotinic receptor (Zwart and Vijverberg, 1998; Nelson et al., 2003) and the trimeric $P2X_{2/6}$ receptor heteromer (Barrera et al., 2007) by manipulating subunit expression levels. No attempt has yet been made to vary the expression levels of, for example, the A- and B-subunits of the 5-HT_3 receptor, leaving open the possibility that its stoichiometry might also be plastic. In fact, it has been reported recently that increasing the relative amounts of cRNA for the δ-subunit in *Xenopus laevis* oocytes expressing the $\alpha_4\beta_3\delta$ receptor caused a progressive decrease in the sensitivity of the receptor to GABA and a corresponding decrease in the Hill slope (You and Dunn, 2007). To account for this observation, it was suggested that the subunit stoichiometry of the $\alpha_4\beta_3\delta$ pentamer might depend on relative subunit expression levels. According to this scenario, one would expect more than one δ-subunit per receptor at high levels of δ-subunit expression.

Our results for the $\alpha_4\beta_3\delta$ $GABA_A$ receptor extend our previous studies on the architecture of ionotropic receptors. The significant technical advance reported here is the method for determining the orientation of the receptor on the mica support, which allows us to solve the structure of receptors containing three different subunits. This method is applicable to other ionotropic receptors and also more widely to other types of multisubunit protein.

TABLE 2
Profile of decoration of $GABA_A$ receptor with Con A and antibody bd17

Number of Particles Bound to Receptor	Con A				Antibody bd17			
	Poly-Lysine	%	Poly-Glutamate	%	Poly-Lysine	%	Poly-Glutamate	%
0	136	88.3	143	79.4	147	91.3	180	82.9
1	12	7.8	27	15.0	14	8.7	32	14.8
2	6	3.9	9	5.0	0	0.0	5	2.3
>2	0	0.0	1	0.6	0	0.0	0	0.0

References

Adkins CE, Pillai GV, Kerby J, Bonnert TP, Haldon C, McKernan RM, Gonzalez JE, Oades K, Whiting PJ, and Simpson PB (2001) $\alpha_4\beta_3\delta$ $GABA_A$ receptors characterized by fluorescence resonance energy transfer-derived measurements of membrane potential. *J Biol Chem* **276:**38934–38939.

Barnard EA, Skolnick P, Olsen RW, Möhler H, Sieghart W, Biggio G, Braestrup C, Bateson AN, and Langer SZ (1998) International Union of Pharmacology. XV. Subtypes of γ-aminobutyric $acid_A$ receptors: classification on the basis of subunit structure and receptor function. *Pharmacol Rev* **50:**291–313.

Barrera NP, Henderson RM, Murrell-Lagnado RD, and Edwardson JM (2007) The stoichiometry of $P2X_{2/6}$ receptor heteromers depends on relative subunit expression levels. *Biophys J* **93:**505–512.

Barrera NP, Herbert P, Henderson RM, Martin IL, and Edwardson JM (2005a) Atomic force microscopy reveals the stoichiometry and subunit arrangement of 5-HT_3 receptors. *Proc Natl Acad Sci U S A* **102:**12595–12600.

Barrera NP, Ormond SJ, Henderson RM, Murrell-Lagnado RD, and Edwardson JM (2005b) AFM imaging demonstrates that $P2X_2$ receptors are trimers, but that $P2X_6$ receptor subunits do not oligomerize. *J Biol Chem* **280:**10759–10765.

Baumann S, Baur R, and Sigel E (2002) Forced subunit assembly in $\alpha_1\beta_2\gamma_2$ $GABA_A$ receptors. *J Biol Chem* **277:**46020–46025.

Baur R, Minier F, and Sigel E (2006) A $GABA_A$ receptor of defined subunit composition and positioning: concatenation of five subunits. *FEBS Lett* **580:**1616–1620.

Bencsits E, Ebert V, Tretter V, and Sieghart W (1999) A significant part of native γ-aminobutyric $acid_A$ receptors containing α_4 subunits do not contain γ or δ subunits. *J Biol Chem* **274:**19613–19616.

Botzolakis EJ, Stanic AK, Feng H-J, Gurba KN, Tian M, and MacDonald RL (2007) Assembly and stoichiometry of $\alpha\beta\delta$ $GABA_A$ receptors. *Soc Neurosci Abstr* **33:**441.3.

Brickley SG, Revilla V, Cull-Candy SG, Wisden W, and Farrant M (2001) Adaptive regulation of neuronal excitability by a voltage-independent potassium conductance. *Nature* **409:**88–92.

Brown N, Kerby J, Bonnert TP, Whiting PJ, and Wafford KA (2002) Pharmacological characterization of a novel cell line expressing human $\alpha_4\beta_3\delta$ $GABA_A$ receptors. *Br J Pharmacol* **136:**965–974.

Chandra D, Jia F, Liang J, Peng Z, Suryanarayanan A, Werner DF, Spigelman I, Houser CR, Olsen RW, Harrison NL, et al. (2006) $GABA_A$ receptor α_4 subunits mediate extrasynaptic inhibition in thalamus and dentate gyrus and the action of gaboxadol. *Proc Natl Acad Sci U S A* **103:**15230–15235.

Connolly CN, Krishek BJ, McDonald BJ, Smart TG, and Moss SJ (1996) Assembly and cell surface expression of heteromeric and homomeric γ-aminobutyric acid type A receptors. *J Biol Chem* **271:**89–96.

Derry JMC, Paulsen IM, Davies M, and Dunn SMJ (2007) A single point mutation of the $GABA_A$ receptor α5-subunit confers fluoxetine sensitivity. *Neuropharmacology* **52:**497–505.

Ernst M, Bruckner S, Boresch S, and Sieghart W (2005) Comparative models of $GABA_A$ receptor extracellular and transmembrane domains: important insights in pharmacology and function. *Mol Pharmacol* **68:**1291–1300.

Farrant M and Nusser Z (2005) Variations on an inhibitory theme: phasic and tonic activation of $GABA_A$ receptors. *Nat Rev Neurosci* **6:**215–229.

Farrar SJ, Whiting PJ, Bonnert TP, and McKernan RM (1999) Stoichiometry of a ligand-gated ion channel determined by fluorescence resonance energy transfer. *J Biol Chem* **274:**10100–10104.

Green WN and Claudio T (1993) Acetylcholine receptor assembly: subunit folding and oligomerization occur simultaneously. *Cell* **74:**57–69.

Im WB, Tai MM, Blakeman DP, and Davis JP (1989) Immobilized $GABA_A$ receptors and their ligand binding characteristics. *Biochem Biophys Res Commun* **163:**611–617.

Karlin A (2002) Emerging structures of the nicotinic acetylcholine receptors. *Nat Rev Neurosci* **3:**102–114.

Karlin A, Holtzman E, Yodh N, Lobel P, Wall J, and Hainfeld J (1983) The arrangement of the subunits of the acetylcholine receptor of *Torpedo californica*. *J Biol Chem* **258:**6678–6681.

Lester HA, Dibas MI, Dahan DS, Leite JF, and Dougherty DA (2004) Cys-loop receptors: new twists and turns. *Trends Neurosci* **27:**329–336.

Lovick TA, Griffiths JL, Dunn SMJ, and Martin IL (2005) Changes in $GABA_A$ receptor subunit expression in the midbrain during the oestrus cycle in Wistar rats. *Neuroscience* **131:**397–405.

Mokrab Y, Bavro VN, Mizuguchi K, Todorov NP, Martin IL, Dunn SMJ, Chan SL, and Chau PL (2007) Exploring ligand recognition and ion flow in comparative models of the human GABA type A receptor. *J Mol Graph Model* **26:**760–774.

Nayeem N, Green TP, Martin IL, and Barnard EA (1994) Quaternary structure of the native $GABA_A$ receptor determined by electron microscopic image analysis. *J Neurochem* **62:**815–818.

Neish CS, Martin IL, Davies M, Henderson RM, and Edwardson JM (2003) Atomic force microscopy of $GABA_A$ receptors bearing subunit-specific tags provides a method for determining receptor architecture. *Nanotechnology* **14:**864–872.

Nelson ME, Kuryatov A, Choi CH, Zhou Y, and Lindstrom J (2003) Alternate stoichiometries of $\alpha4\beta2$ nicotinic acetylcholine receptors. *Mol Pharmacol* **63:**332–341.

Nusser Z and Mody I (2002) Selective modulation of tonic and phasic inhibitions in dentate gyrus granule cells. *J Neurophysiol* **87:**2624–2628.

Nusser Z, Sieghart W, and Somogyi P (1998) Segregation of different $GABA_A$ receptors to synaptic and extrasynaptic membranes of cerebellar granule cells. *J Neurosci* **18:**1693–1703.

Richards JG, Schoch P, Häring P, Takacs B, and Möhler H (1987) Resolving $GABA_A$/benzodiazepine receptors: cellular and subcellular localization in the CNS with monoclonal antibodies. *J Neurosci* **7:**1866–1886.

Schneider SW, Lärmer J, Henderson RM, and Oberleithner H (1998) Molecular weights of individual proteins correlate with molecular volumes measured by atomic force microscopy. *Pflugers Arch* **435:**362–367.

Schwarzer C, Tsunashima K, Wanzenbock C, Fuchs K, Sieghart W, and Sperk G (1997) $GABA_A$ receptor subunits in the rat hippocampus II: altered distribution in kainic acid-induced temporal lobe epilepsy. *Neuroscience* **80:**1001–1017.

Shen H, Gong QH, Aoki C, Yuan M, Ruderman Y, Dattilo M, Williams K, and Smith SS (2007) Reversal of neurosteroid effects at $\alpha4\beta2\delta$ $GABA_A$ receptors triggers anxiety at puberty. *Nat Neurosci* **10:**469–477.

Sieghart W (1995) Structure and pharmacology of gamma-aminobutyric $acid_A$ receptor subtypes. *Pharmacol Rev* **47:**181–234.

Stell BM, Brickley SG, Tang CY, Farrant M, and Mody I (2003) Neuroactive steroids reduce neuronal excitability by selectively enhancing tonic inhibition mediated by δ subunit-containing $GABA_A$ receptors. *Proc Natl Acad Sci U S A* **100:**14439–14444.

Stórustovu S and Ebert B (2006) Pharmacological characterization of agonists at δ-containing $GABA_A$ receptors: functional selectivity for extrasynaptic receptors is dependent on the absence of γ_2. *J Pharmacol Exp Ther* **316:**1351–1359.

Venturoli D and Rippe B (2005) Ficoll and dextran vs. globular proteins as probes for testing glomerular permselectivity: effects of molecular size, shape, charge, and deformability. *Am J Physiol Renal Physiol* **288:**F605–F613.

You H and Dunn SMJ (2007) Identification of a domain in the δ subunit (S238–V264) of the $\alpha_4\beta_3\delta$ $GABA_A$ receptor that confers high agonist sensitivity. *J Neurochem* **103:**1092–1101.

Zhang N, Wei W, Mody I, and Houser CR (2007) Altered localisation of $GABA_A$ receptor subunits on dentate granule cell dendrites influences tonic and phasic inhibition in a mouse model of epilepsy. *J Neurosci* **27:**7520–7531.

Zwart R and Vijverberg HPM (1998) Four pharmacologically distinct subtypes of $\alpha_4\beta_2$ nicotinic acetylcholine receptor expressed in *Xenopus laevis* oocytes. *Mol Pharmacol* **54:**1124–1131.

Address correspondence to: J. Michael Edwardson, Department of Pharmacology, University of Cambridge, Tennis Court Road, Cambridge CB2 1PD, United Kingdom. E-mail: jme1000@cam.ac.uk